Available online at www.sciencedirect.com
SCIENCE DIRECT®
Journal of Solid State Chemistry 174 (2003) 152–158
JOURNAL OF SOLID STATE CHEMISTRY
http://elsevier.com/locate/jssc

Synthesis, crystal structure and magnetic properties of $U_2Co_6Al_{19}$

O. Tougait,[a,*] J. Stêpieň-Damm,[b] V. Zaremba,[c] H. Noël,[a] and R. Troc[b]

[a] *Laboratoire de Chimie du Solide et Inorganique Moléculaire, UMR 6511 CNRS-Université de Rennes1, Avenue du Général Leclerc, 35042 Rennes, France*

[b] *W. Trzebiatowski, Institute of Low Temperature and Structure Research, 50-950 Wrocław, P.O. Box 1410, Poland*

[c] *Department of Inorganic Chemistry, I. Franko L'viv National University, Kyryla and Mefodiya Str. 6, 79005 L'viv, Ukraine*

Received 26 December 2002; received in revised form 17 March 2003; accepted 31 March 2003

Abstract

The new compound $U_2Co_6Al_{19}$ was prepared by reaction of the elemental components in an arc-melting furnace followed by a heat treatment at 1050°C for 500 h. Its chemical composition was checked by energy-dispersive X-ray analyses and its crystal structure was determined by single crystal X-ray diffraction experiments. It crystallizes with four formula units in the monoclinic space group $C2/m$ in a unit cell of dimensions $a = 17.4617(3)$ Å, $b = 12.0474(2)$ Å, $c = 8.2003(1)$ Å, $\beta = 103.915(1)^\circ$. The crystal structure of $U_2Co_6Al_{19}$ can be regarded as a superstructure of $NdCo_{4-x}Ga_9$ structure type. This complex structure consists of a three-dimensional Co–Al framework delimiting tunnels where the U atoms reside. The shortest U–U distances are found in the c direction with alternating values of 3.98(1) and 4.22(1) Å. Temperature-dependent magnetization shows a first peak at 12.5 K and a weak ferromagnetic character below the temperature $T_C = 8$ K. Magnetization at 1.9 K reaches almost saturation in 5 T with the moment of 0.36 μ_B/U atom. The complex magnetic behavior of $U_2Co_6Al_{19}$ may be ascribed to a canted spin structure resulting from an antiparallel arrangement of the magnetic moments not fully compensated at low temperature. At higher temperature, the compound displays simple paramagnetic behavior.

Keywords: Uranium alloy; Polyaluminide; Superstructure; Phase diagram; Complex magnetic behavior

1. Introduction

During the past three decades, U-based intermetallic compounds have been revealed to be a continuous source of materials for the study of unusual physical properties. They may exhibit a wide variety of electronic phenomena including heavy fermion behavior, Kondo effect, valence fluctuation, coexistence of magnetism and superconductivity, which still constitutes an important challenge for theory. However, there is increasing evidence that the ground state properties of these strongly correlated electron systems are substantially altered and even governed by a moderate crystallographic disorder [1–3]. This is the reason why, prior to detailed studies of their physical properties, a sound structural and chemical characterization of the investigated materials is essential.

As part of our research program on new compounds, we have undertaken a systematic study of the U–Co–Al ternary system. At the initial stages of this investigation, we have identified a ternary compound with a chemical formula close to UCo_3Al_{9+x} that we had considered as crystallizing with the $NdCo_{4-x}Ga_9$ structure type [4]. This structure presented a disorder with one 8 h Wyckoff position of the *Imma* (no. 74) space group partially occupied by an Al atom, whereas in the gallide compound, this crystallographic position is partially occupied by a Co atom. Subsequent single crystal X-ray diffraction experiments using a four-circle diffractometer equipped with a CCD camera reveal that the phase initially identified as UCo_3Al_{9+x} presents a superstructure leading to a well-ordered structure that must be formulated as $U_2Co_6Al_{19}$. In this paper, we report the determination of the superstructure of $U_2Co_6Al_{19}$ as well as its basic magnetic properties.

2. Experimental

2.1. Syntheses and characterizations

Initial investigations were carried out in the ternary U–Co–Al system by analyzing arc-melted ingots with

*Corresponding author. Fax: +33-2-99-38-34-87.
E-mail address: tougait@univ-rennes1.fr (O. Tougait).

0022-4596/03/$ - see front matter © 2003 Published by Elsevier Science (USA).
doi:10.1016/S0022-4596(03)00191-9

diverse starting compositions. After a proper characterization of the composition of the title compound, pure samples were prepared by reaction of the elements in the atomic ratio U:Co:Al of 2:6:19, melted in an arc-furnace under purified argon atmosphere. The cooled buttons were flipped and remelted three times to achieve homogeneity. The weight losses were less than 1 wt%. Each sample was placed into an alumina crucible and sealed in a fused silica tube under a residual atmosphere of argon. The reaction tubes were heated at a rate of 60°C/h to 1050°C, held there for 500 h, followed by a rapid cooling to room temperature.

Metallographic and quantitative analyses (EDX) were obtained with the use of a 6400-JSM scanning electron microscope equipped with an Oxford Link Isis spectrometer. A piece of each sample was mounted in resin and thoroughly polished before examination. Through the use of stoichiometric compounds such as UAl_2, UCo_2 and Co_2Al_5 as external standards, additional corrections were superimposed as the internal ZAF corrections. All samples were analyzed by powder X-ray diffraction patterns collected on an INEL CPS 120 diffractometer working with monochromatized Cu$K\alpha_1$ radiation.

The single crystal used for the structure refinement of the substructure was selected from an arc-melted ingot with a starting composition of U:Co:Al of 1:4:12. The X-ray diffraction data were collected at room temperature with a Kuma KM-4 CCD diffractometer using monochromatized Mo$K\alpha$ radiation. Data reduction, excluding weak reflections, was performed using KM-4 Data-Red program.

The single crystal used for the refinement of the superstructure was manually selected from a sample with starting composition U:Co:Al of 1:1:8, heat treated at 1050°C for 300 h. The X-ray diffraction experiments were carried out with a Nonius Kappa CCD diffractometer using a graphite-monochromatized Mo$K\alpha$ radiation. The unit-cell parameters, orientation matrix as well as the control of the crystal quality were derived from 10 frames recorded at $\phi = 0$ using a scan of 1° in ω. The complete strategy to fill more than a hemisphere of the reciprocal sphere was automatically calculated with the use of the program COLLECT [5]. Data reduction and reflection indexing were performed with the program DENZO of the Kappa CCD software package [5]. The scaling and merging of redundant measurements of the different data sets as well as the cell refinement was performed using DENZO. The data were corrected for absorption using a semi-empirical method [6] which is based on redundant and equivalent reflections. Most of the atoms of the structure were located by direct methods using SIR-97 [7]. All structure refinements and Fourier syntheses were carried out with the help of SHELXL-97 [8].

Magnetic measurements were carried out using a MPMS Quantum Design SQUID magnetometer. The temperature dependence of the magnetization was measured in the range 1.9–400 K under a magnetic field of 0.5 T. The isothermal variation of the magnetization was measured at 1.9 K under applied fields up to 5 T.

3. Results and discussion

3.1. Crystal structure determination

The initial crystallographic study of the new ternary compound led to its characterization in the body-centered orthorhombic system with unit-cell parameters $a = 4.110(1)$ Å, $b = 12.052(2)$ Å, $c = 16.985(3)$ Å. Its chemical formula deduced from the single crystal refinement was UCo_3Al_{9+x} with x close to 0.5. It was thus considered that this new ternary compound crystallized with the $NdCo_{4-x}Ga_9$ structure type [4]. The difference between the two crystal structures is that one 8*h* Wyckoff position is partially occupied by a Co atom in the gallide, whereas this crystallographic site is partially occupied by an Al atom in the aluminide. The EDX results confirmed the composition UCo_3Al_{9+x} with x close to 0.5. Moreover, no solubility range could be detected on the Al composition. Thus, these observations alerted us to the possibility of a superstructure. Close examination of reconstruction of precession pictures reveals weak reflections that could not be indexed in the body-centered orthorhombic unit-cell (Fig. 1).

A larger single crystal with dimensions of $0.045 \times 0.040 \times 0.030\,mm^3$ was used for the second crystallographic study carried out on a Nonius Kappa

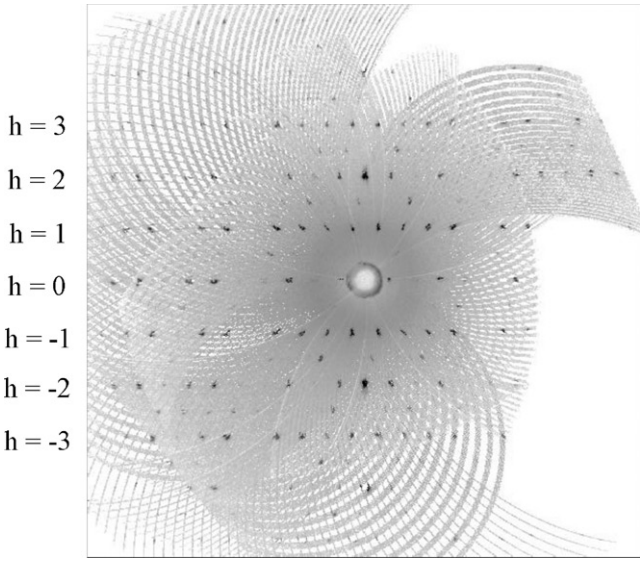

Fig. 1. Reconstruction of the *h*0l precession picture in the body-centered orthorhombic unit cell showing clearly weak reflections with non-integer indices.

CCD diffractometer. The intensities of the additional reflections were strong enough to allow the determination of the unit cell of the superstructure as well as the crystal structure refinement. All the reflections could be indexed in a face-centered monoclinic lattice, with its parameters related to those of the orthorhombic subcell by $\vec{a}_{super} = -\vec{a}_{sub} + \vec{c}_{sub}$, $\vec{b}_{super} = -\vec{b}_{sup}$, $2 \times \vec{a}_{sub}$, giving a β angle of 103.92(1)°. The positions of the U atoms, Co atoms and ten Al atoms were correctly determined by direct methods. The position of the last Al atom was located from difference electron density synthesis. The isotropic atomic displacement parameter of Al(1) is found to be about four times higher than those of the other Al atoms. In subsequent least-squares cycles, the occupancy parameter of Al(1) was allowed to vary. No deviation of the full occupancy was observed. A splitting of this position was also attempted, yielding an unstable refinement. Furthermore, the Fourier map in the vicinity of Al(1) is flat and the ten first residual peaks are located close to U(1) and U(2) positions. Therefore, only a weak "rattling" of Al(1) over its atomic position is expected. The final refinements included a secondary extinction and anisotropic atomic displacement parameters for all atoms. The determination of the crystal structure in the monoclinic *C*-centered unit cell leads to a perfectly ordered structure. The superstructure results from an ordering of the Al atoms. Crystallographic details are summarized in Table 1. Atomic coordinates and equivalent atomic displacement parameters, with their standard deviations are given in Table 2. Selected interatomic distances are provided in Table 3.

The same superstructure model was found for several single crystals, from both annealed and as-cast alloys, using the data collected on Nonius Kappa CCD diffractometer and on Xcalibur CCD diffractometer. A similar structure was also recently observed for the new ternary compounds $Th_2Co_6Al_{19}$ and $Ce_2Co_6Al_{19}$.

Table 1
Crystal data and structure refinement for $U_2Co_6Al_{19}$

Empirical formula	$U_2Co_6Al_{19}$
Formula weight (g/mol)	1342.26
Crystal system, space group	Monoclinic, $C2/m$ (no. 12)
Unit cell dimensions (Å, °)	$a = 17.4617(3)$, $\alpha = 90$
	$b = 12.0474(2)$, $\beta = 103.915(1)$
	$c = 8.2003(1)$, $\gamma = 90$
Volume (Å^3)	1674.46(4)
Z, Calculated density (g/cm^3)	4, 5.324
Absorption coefficient (cm^{-1})	260.4
Crystal color and habit	Black, prism
Crystal size (mm^3)	$0.045 \times 0.040 \times 0.030$
Theta range for data collection (°)	2.07–37.09
Limiting indices	$-29 \leqslant h \leqslant 24$
	$-20 \leqslant k \leqslant 19$
	$-13 \leqslant l \leqslant 13$
Reflections collected/unique	26867/4429
R(int)	0.0935
Absorption correction	Semi-empirical from equivalents
Max./min. transmission	0.397/0.268
Data/restraints/parameters	4429/0/133
Goodness-of-fit on F^2	1.062
R indices[a] $[I > 2\sigma(I)]$	$R(F) = 0.0395$,
	$wR_2 = 0.0950$
R indices[a] (all reflections)	$R(F) = 0.0563$,
	$wR_2 = 0.1033$
Extinction coefficient	0.00150(7)
Largest diff. peak and hole (e. Å^{-3})	5.989 and −5.186

[a] $R(F) = \sum||F_0| - |F_c||/|F_c|$, $wR_2 = \left[\sum w(F_0^2 - F_c^2)^2 / wF_c^4\right]^{1/2}$, where $w^{-1} = \sigma^2(F_0^2) + (0.05F_0^2)^2$ for $F_0^2 \geqslant 0$ and $w^{-1} = \sigma^2(F_0^2)$ for $F_0^2 < 0$.

Table 2
Atomic coordinates and equivalent isotropic displacement parameters (Å^2) for $U_2Co_6Al_{19}$

Atom	Wyckoff site	x	y	z	U_{eq}. (Å^2)
U(1)	4*i*	0.2811(1)	0	0.2577(1)	0.008(1)
U(2)	4*i*	0.7182(1)	0	0.2273(1)	0.008(1)
Co(1)	4*i*	0.4350(1)	0	0.0923(1)	0.007(1)
Co(2)	4*i*	0.5631(1)	0	0.4063(1)	0.007(1)
Co(3)	8*j*	0.1209(1)	0.1983(1)	0.1890(1)	0.007(1)
Co(4)	8*j*	0.3837(1)	0.3032(1)	0.3271(1)	0.008(1)
Al(1)	4*g*	0	0.1685(2)	0	0.039(1)
Al(2)	4*i*	0.0827(1)	0	0.6494(3)	0.013(1)
Al(3)	4*i*	0.0886(1)	0	0.1824(2)	0.011(1)
Al(4)	8*j*	0.0263(1)	0.1719(1)	0.3623(2)	0.015(1)
Al(5)	8*j*	0.0522(1)	0.3812(1)	0.1542(2)	0.008(1)
Al(6)	8*j*	0.1487(1)	0.3326(1)	0.4483(2)	0.009(1)
Al(7)	8*j*	0.1827(1)	0.1150(1)	0.4664(2)	0.008(1)
Al(8)	8*j*	0.2522(1)	0.2506(1)	0.2416(1)	0.010(1)
Al(9)	8*j*	0.3326(1)	0.3875(1)	0.0450(2)	0.011(1)
Al(10)	8*j*	0.3591(1)	0.1742(1)	0.0543(2)	0.010(1)
Al(11)	8*j*	0.4459(1)	0.1179(1)	0.3510(2)	0.008(1)

U_{eq} is defined as one-third of the trace of the orthogonalized U_{ij} tensor.

Table 3
Selected interatomic distances (Å) for $U_2Co_6Al_{19}$

U(1)–Al(7) × 2	3.035(2)	U(2)–Al(7) × 2	3.021(2)	Co(1)–Al(5) × 2	2.448(2)
U(1)–Al(8) × 2	3.059(2)	U(2)–Al(8) × 2	3.059(2)	Co(1)–Al(10) × 2	2.461(2)
U(1)–Al(9) × 2	3.094(2)	U(2)–Al(9) × 2	3.081(2)	Co(1)–Al(11) × 2	2.522(2)
U(1)–Al(11) × 2	3.135(2)	U(2)–Al(6) × 2	3.144(2)	Co(1)–Al(5) × 2	2.531(2)
U(1)–Al(6) × 2	3.156(2)	U(2)–Al(5) × 2	3.159(2)	Co(1)–Co(2)	2.977(2)
U(1)–Al(10) × 2	3.183(2)	U(2)–Al(10) × 2	3.171(2)	Co(1)–Co(1)	3.017(1)
U(1)–Al(3)	3.269(2)	U(2)–Al(2)	3.379(2)	Co(1)–U(2)	3.264(2)
U(1)–Co(1)	3.288(1)	U(2)–Co(1)	3.264(2)	Co(1)–U(1)	3.288(1)
Co(2)–Al(11) × 2	2.442(2)	Co(3)–Al(8)	2.315(2)	Co(4)–Al(8)	2.323(2)
Co(2)–Al(11) × 2	2.481(2)	Co(3)–Al(1)	2.327(1)	Co(4)–Al(2)	2.439(1)
Co(2)–Al(5) × 2	2.484(2)	Co(3)–Al(4)	2.446(2)	Co(4)–Al(4)	2.454(2)
Co(2)–Al(6) × 2	2.485(2)	Co(3)–Al(3)	2.453(1)	Co(4)–Al(11)	2.469(2)
Co(2)–Co(2)	2.974(2)	Co(3)–Al(9)	2.482(2)	Co(4)–Al(7)	2.477(2)
Co(2)–Co(1)	2.977(2)	Co(3)–Al(7)	2.483(2)	Co(4)–Al(9)	2.487(2)
Co(2)–U(1)	3.374(2)	Co(3)–Al(5)	2.492(2)	Co(4)–Al(6)	2.625(2)
Co(2)–U(2)	3.378(1)	Co(3)–Al(10)	2.607(2)	Co(4)–Al(4)	2.669(2)
		Co(3)–Al(6)	2.622(2)	Co(4)–Al(10)	2.673(2)
Al(1)–Co(3) × 2	2.327(1)	Al(2)–Co(4) × 2	2.439(1)	Al(3)–Co(3) × 2	2.4527(7)
Al(1)–Al(3) × 2	2.764(2)	Al(2)–Al(4) × 2	2.798(2)	Al(3)–Al(1) × 2	2.764(2)
Al(1)–Al(4) × 2	2.895(2)	Al(2)–Al(7) × 2	2.913(2)	Al(3)–Al(7) × 2	2.864(2)
Al(1)–Al(5) × 2	2.905(2)	Al(2)–Al(9) × 2	2.919(2)	Al(3)–Al(4) × 2	2.902(2)
Al(2)–Al(9) × 2	3.107(2)	Al(2)–Al(4) × 2	3.113(2)	Al(3)–Al(9) × 2	2.906(2)
		Al(2)–U(2)	3.379(2)	Al(3)–U(1)	3.269(2)
Al(4)–Co(3)	2.446(2)	Al(5)–Co(1)	2.448(2)	Al(6)–Co(2)	2.485(2)
Al(4)–Co(4)	2.454(2)	Al(5)–Co(3)	2.484(2)	Al(6)–Co(3)	2.622(2)
Al(4)–Al(4)	2.635(3)	Al(5)–Co(2)	2.492(2)	Al(6)–Co(4)	2.625(2)
Al(4)–Co(4)	2.669(2)	Al(5)–Co(1)	2.531(2)	Al(6)–Al(5)	2.654(2)
Al(4)–Al(7)	2.746(2)	Al(5)–Al(6)	2.654(2)	Al(6)–Al(11)	2.665(2)
Al(4)–Al(2)	2.798(2)	Al(5)–Al(10)	2.654(2)	Al(6)–Al(7)	2.684(2)
Al(4)–Al(6)	2.844(2)	Al(5)–Al(11)	2.736(2)	Al(6)–Al(4)	2.844(2)
Al(4)–Al(11)	2.885(2)	Al(5)–Al(5)	2.739(3)	Al(6)–Al(8)	2.890(2)
Al(4)–Al(1)	2.895(2)	Al(5)–Al(5)	2.863(3)	Al(6)–Al(7)	2.926(2)
Al(4)–Al(3)	2.902(2)	Al(5)–Al(1)	2.905(2)	Al(6)–Al(8)	2.930(2)
Al(4)–Al(2)	3.113(2)	Al(5)–Al(4)	3.137(2)	Al(6)–U(2)	3.144(2)
Al(4)–Al(5)	3.137(2)	Al(5)–U(2)	3.159(2)	Al(6)–U(1)	3.156(2)
Al(7)–Co(4)	2.477(2)	Al(8)–Co(3)	2.315(2)	Al(9)–Co(3)	2.482(2)
Al(7)–Co(3)	2.483(2)	Al(8)–Co(4)	2.323(2)	Al(9)–Co(4)	2.487(2)
Al(7)–Al(6)	2.684(2)	Al(8)–Al(10)	2.841(2)	Al(9)–Al(10)	2.610(2)
Al(7)–Al(4)	2.746(2)	Al(8)–Al(10)	2.866(2)	Al(9)–Al(9)	2.710(3)
Al(7)–Al(7)	2.770(3)	Al(8)–Al(7)	2.888(2)	Al(9)–Al(8)	2.895(2)
Al(7)–Al(3)	2.864(2)	Al(8)–Al(6)	2.890(2)	Al(9)–Al(3)	2.906(2)
Al(7)–Al(8)	2.888(2)	Al(8)–Al(9)	2.895(2)	Al(9)–Al(2)	2.919(2)
Al(7)–Al(2)	2.913(2)	Al(8)–Al(6)	2.930(2)	Al(9)–Al(8)	2.968(2)
Al(7)–Al(6)	2.926(2)	Al(8)–Al(7)	2.935(2)	Al(9)–Al(1)	3.107(2)
Al(7)–Al(8)	2.935(2)	Al(8)–Al(9)	2.968(2)	Al(9)–U(2)	3.081(2)
Al(7)–U(2)	3.021(2)	Al(8)–U(1)	3.059(2)	Al(9)–U(1)	3.094(2)
Al(7)–U(1)	3.035(2)	Al(8)–U(2)	3.059(2)		
Al(10)–Co(1)	2.461(2)	Al(11)–Co(2)	2.442(2)		
Al(10)–Co(3)	2.607(2)	Al(11)–Co(4)	2.469(2)		
Al(10)–Co(4)	2.673(2)	Al(11)–Co(2)	2.481(2)		
Al(10)–Al(9)	2.610(2)	Al(11)–Co(1)	2.522(2)		
Al(10)–Al(11)	2.628(2)	Al(11)–Al(10)	2.628(2)		
Al(10)–Al(5)	2.654(2)	Al(11)–Al(6)	2.665(2)		
Al(10)–Al(8)	2.841(2)	Al(11)–Al(11)	2.705(3)		
Al(10)–Al(8)	2.866(2)	Al(11)–Al(5)	2.736(2)		
Al(10)–U(2)	3.171(2)	Al(11)–Al(11)	2.842(3)		
Al(10)–U(1)	3.183(2)	Al(11)–Al(4)	2.885(2)		
		Al(11)–U(1)	3.135(2)		

3.2. Crystal structure description

The interatomic distances found in $U_2Co_6Al_{19}$ compare well with those reported for the binary polyaluminide compounds such as UAl_4 [9], Co_2Al_5 [10] and Co_2Al_9 [11]. A comparison of the interatomic distances with the sum of the atomic radii ($r_{Co}=1.25$ Å, $r_{Al}=1.43$ Å and $r_U=1.53$ Å) reveals that most of the Al–Al distances and all the Co–Al distances are shorter than the sum of the atomic radii, whereas the U–Co and U–Al distances are longer than the sum of the atomic radii. The Co–Al and Al–Al distances range from 2.315(2) to 2.673(2) Å and from 2.610(2) to 3.137(2) Å, respectively, suggesting a dominant covalent character of the chemical bonds. Therefore, the Co–Al and Al–Al contacts can be described as strong bonding interactions. The U–Al and U–Co distances range from 3.021(2) to 3.379(2) Å and from 3.264(2) to 3.288(1) Å, respectively, reflecting rather weak bonding interactions between the U atoms and their near-neighbors.

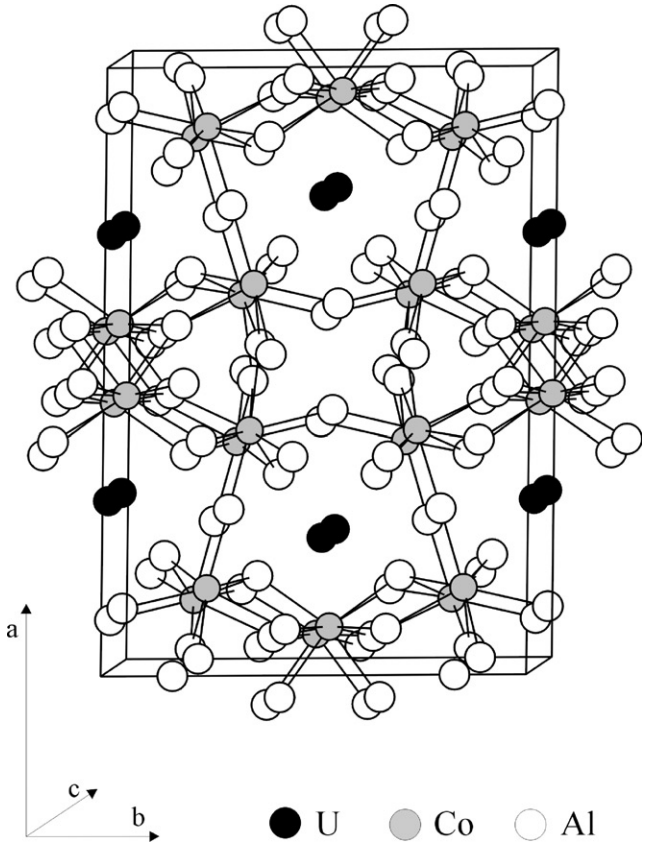

Fig. 2. Perspective view of the structure of $U_2Co_6Al_{19}$ down the *c*-axis. For clarity, the bonds around U atoms have been removed.

Fig. 2 displays a perspective view of $U_2Co_6Al_{19}$ down the *c*-axis. The crystal structure is a complicated three-dimensional network that shows extensive Co–Al and Al–Al contacts. To simplify, the structure of $U_2Co_6Al_{19}$ can be viewed as a Co–Al framework delimiting apparently pentagonal channels where the U atoms reside.

The coordination spheres around the Co atoms are of two geometries and involve either a pure Al environment or a mixed environment of U/Co/Al. Co(1) and Co(2) atoms have a coordination number of 12 with 8 Al forming a distorted square prism having its four rectangular faces capped by two U atoms and two Co atoms (Fig. 3a). The square prisms centered by Co(1) and Co(2) pack by face-sharing to form along the *c*-axis a fluorite-like slab. Co(3) and Co(4) atoms are surrounded by 9 Al atoms in a tricapped trigonal prismatic geometry (Fig. 3b). Along the *c*-axis, they share their triangular faces to form an infinite column of prisms. In the $a-b$ plane, they share two common Al atoms, namely Al(4) and Al(8) to form infinite corrugated chains. Finally, the three-dimensional Co–Al framework is constructed by edge sharing between the different columns and slabs. The connection also defines tunnels with roughly pentagonal section where the U atoms are located.

The coordination sphere of the uranium atoms consists of 13 Al atoms and one additional Co atom (Fig. 3c). The motif comprises a strongly distorted rectangular prism of 8 Al atoms having an equatorial pentagonal ring of 5 Al. The connection between two adjacent polyhedra centered by U(1) and U(2) occurs by

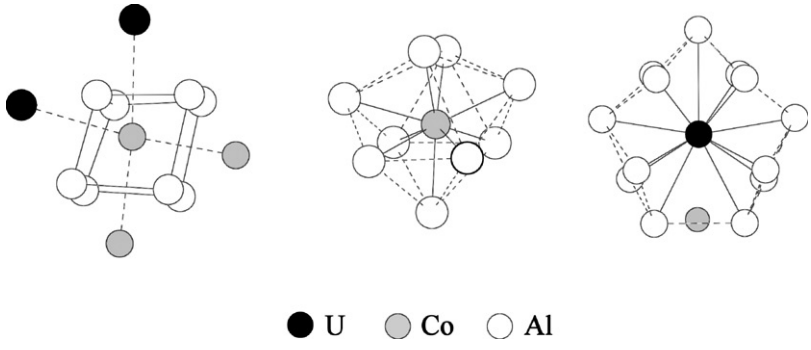

Fig. 3. (a) Distorted square prism of 8 Al along with the capping atoms found around Co(1) and Co(2). (b) Tricapped trigonal prism of Al atoms found around Co(3) and Co(4). (c) Coordination polyhedron found around the U atoms.

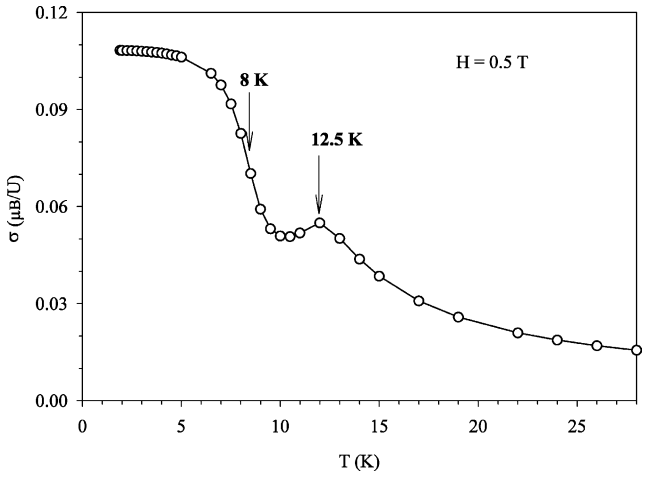

Fig. 4. Low-temperature details of the magnetization curve.

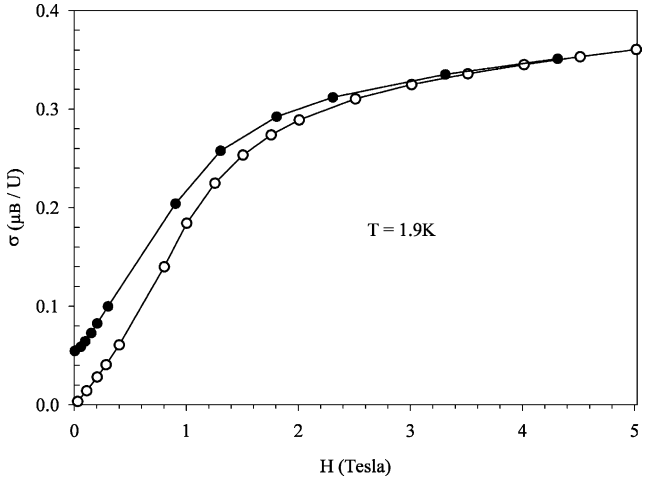

Fig. 5. Magnetization (σ) versus magnetic field performed at 1.9 K.

sharing their rectangular faces along the *c*-axis. It results that the shortest U–U distances are found in the *c*-direction with alternating values of 3.98(1) and 4.22(1) Å.

3.3. Magnetic properties

Only some preliminary studies of magnetic properties have been performed and are presented here. Fig. 4 shows the magnetization σ measured under an applied field of 0.5 T covering the range of temperature 1.9–28 K. In this low-temperature region, the magnetization passes through a weak peak at 12.5 K, signaling an antiferromagnetic order. Upon cooling, the magnetization increases and saturates to 0.11 μ_B/U atom. The observed inflection point at 8 K suggests the presence of possible transition to a weak ferromagnetism, which can be caused by the deviation from an antiparallel arrangement of the magnetic moments in this low-symmetry structure. Similar transition temperatures were derived from the temperature variation of the electrical resistivity, which will be a subject of a separate report [12].

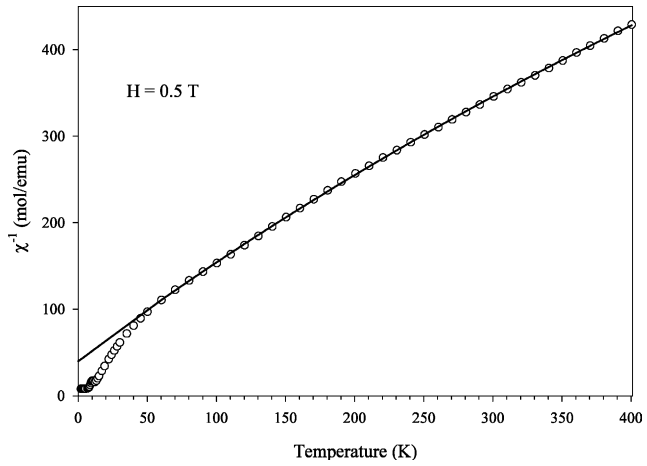

Fig. 6. Inverse magnetic susceptibility of $U_2Co_6Al_{19}$ in the temperature range 1.9–400 K. The solid line represents the fit of the data to the modified Curie–Weiss law.

Fig. 5 presents the magnetization curve measured at 1.9 K with increasing and decreasing fields up to 5 T. At this field the magnetization curve is close to saturation and reaches a value of 0.36 μ_B/U atom. A small hysteresis in the magnetization yields a remanence of 0.06 μ_B/U atom.

In the paramagnetic state, the reciprocal susceptibility versus temperature dependence is curvilinear with rapid decrease toward the temperature axis below about 200 K and being almost straight line above this temperature (Fig. 6). Such a variation of the reciprocal susceptibility is rather reminiscent of ferrimagnetic type of behavior. A fit of the magnetic susceptibility to the modified Curie Weiss law, made in the range of temperature 60–400 K yields an effective magnetic moment of uranium $\mu_{eff} = 2.5\,\mu_B$/U atom, a paramagnetic Curie temperature $\theta_p = -34$ K and an independent term of the Pauli paramagnetism $\chi_0 = 0.0005$ emu/mol.

Acknowledgments

This work was partially supported by the exchange program between CNRS and Polish Academy of Sciences, under the project 6386. Use was made of the Nonius Kappa CCD diffractometer through the Centre de Diffraction X de l'Université de Rennes1 (CDIFX).

References

[1] E. Miranda, V. Dobrosavljevich, G. Kotliar, Phys. Rev. Lett. 78 (1997) 290.

[2] A.H. Castro Neto, G.E. Castilla, B. Alones, Phys. Rev. Lett. 81 (1998) 3531.
[3] S. Süllow, M.B. Maple, D. Tornuta, G.J. Nieuwenhuys, A.A. Menovsky, J.A. Mydosh, R. Chau, J. Magn. Magn. Mater. 226/230 (2001) 35.
[4] O.I. Moroz, G.E. Stetskovich, O.M. Sichevich, Yu.N. Grin, Ya.P. Yarmolyuk, Sov. Phys. Crystallogr. 28 (1983) 470.
[5] Nonius, in: Collect, Denzo, Scalepack, Sortav. Kappa CCD Program Package, Nonius BV, Delft, The Netherlands, 1998.
[6] R.H. Blessing, Acta Crystallogr. A 51 (1995) 33.
[7] A. Altomare, M.C. Burla, M. Camalli, G.L. Cascarano, C. Giacovazzo, A. Guagliardi, A.G.G. Moliterni, G. Polidori, R. Spagna, J. Appl. Crystallogr. 32 (1999) 115.
[8] G.M. Sheldrick, Shelxs97 and Shelxl97, University of Göttingen, Germany.
[9] B.S. Borie, Trans. AIME 191 (1951) 800.
[10] J.B. Newkirk, P.J. Black, A. Damjavonic, Acta Crystallogr. 14 (1961) 532.
[11] A.M.B. Douglas, Acta Crystallogr. 3 (1950) 19.
[12] R. Troc, et al., to be published.